Mechanisms of Signal Transduction:

Indole-3-Carbinol (I3C) Inhibits Cyclin-dependent Kinase-2 Function in Human Breast Cancer Cells by Regulating the Size Distribution, Associated Cyclin E Forms, and Subcellular Localization of the CDK2 Protein Complex

Hanh H. Garcia, Gloria A. Brar, David H. H. Nguyen, Leonard F. Bjeldanes and Gary L. Firestone

J. Biol. Chem. 2005, 280:8756-8764.
doi: 10.1074/jbc.M407957200 originally published online December 20, 2004

THE JOURNAL OF BIOLOGICAL CHEMISTRY
Vol. 280, No. 10, Issue of March 11, pp. 8756–8764, 2005
Printed in U.S.A.

Indole-3-Carbinol (I3C) Inhibits Cyclin-dependent Kinase-2 Function in Human Breast Cancer Cells by Regulating the Size Distribution, Associated Cyclin E Forms, and Subcellular Localization of the CDK2 Protein Complex*

Received for publication, July 14, 2004, and in revised form, December 15, 2004
Published, JBC Papers in Press, December 20, 2004, DOI 10.1074/jbc.M407957200

Hanh H. Garcia‡§, Gloria A. Brar‡, David H. H. Nguyen‡, Leonard F. Bjeldanes¶, and Gary L. Firestone‡‖

From the ‡Department of Molecular and Cell Biology and The Cancer Research Laboratory and the ¶Department of Nutritional Sciences and Toxicology, The University of California at Berkeley, Berkeley, California 94720

Indole-3-carbinol (I3C), a dietary compound found in cruciferous vegetables, induces a robust inhibition of CDK2 specific kinase activity as part of a G_1 cell cycle arrest of human breast cancer cells. Treatment with I3C causes a significant shift in the size distribution of the CDK2 protein complex from an enzymatically active 90 kDa complex to a larger 200 kDa complex with significantly reduced kinase activity. Co-immunoprecipitations revealed an increased association of both a 50 kDa cyclin E and a 75 kDa cyclin E immunoreactive protein with the CDK2 protein complex under I3C-treated conditions, whereas the 90 kDa CDK2 protein complexes detected in proliferating control cells contain the lower molecular mass forms of cyclin E. I3C treatment caused no change in the level of CDK2 inhibitors (p21, p27) or in the inhibitory phosphorylation states of CDK2. The effects of I3C are specific for this indole and not a consequence of the cell cycle arrest because treatment of MCF-7 breast cancer cells with either the I3C dimerization product DIM or the anti-estrogen tamoxifen induced a G_1 cell cycle arrest with no changes in the associated cyclin E or subcellular localization of the CDK2 protein complex. Taken together, our results have uncovered a unique effect of I3C on cell cycle control in which the inhibition of CDK2 kinase activity is accompanied by selective alterations in cyclin E composition, size distribution, and subcellular localization of the CDK2 protein complex.

Considerable epidemiological evidence show that diets high in vegetable and fiber lead to low cancer risks and confer protection from various forms of cancers, including breast cancer (1, 2). In particular, consumption of vegetables belonging to the Brassica genus, which includes broccoli, cabbage, and cauliflower, have been reported to correlate with a decrease in mammary tumor incidence (3). These epidemiological studies suggest the existence of naturally occurring compounds in dietary sources that represent a largely untapped source of potential chemotherapeutic molecules. One such phytochemical is indole-3-carbinol (I3C),[1] an autolysis product of gluccosinolates present in Brassica vegetables. Dietary exposure to I3C reduced tumor occurrence and decreased the multiplicity of spontaneous as well as carcinogen-induced mammary tumor formation in rodent model systems (4–8). Furthermore, diets high in cabbage, a good source of I3C, reduced pulmonary metastasis of mammary tumor implants in mice (9). Consistent with these studies, I3C tested positive as a chemopreventative agent in several short term bioassays relevant to carcinogen-induced DNA damage, tumor initiation and promotion, and oxidative stress (10).

When ingested, the low pH environment of the stomach converts a large fraction of I3C into a variety of natural indole oligomers (11–15), such as its diindole products 3,3′-diindolylmethane (DIM), and indole[3,2-b]carbazole, which account for many of the *in vivo* anti-estrogenic and anti-tumorigenic biological activities of I3C (14). In contrast to this dietary pathway, emerging evidence has revealed that I3C also exhibits direct anti-proliferative activity on certain cancer cells. One study showed that ectopic application of I3C directly inhibits skin tumor formation in mouse models (17). Studies by us (18–27) and by others (24, 25, 28–33) have shown that I3C has both anti-proliferative and/or apoptotic effects on cultured human reproductive cancer cells depending on the dose used in the assay.

Regulated changes in the expression and/or activity of G_1 cell cycle components control the growth of normal mammary epithelial cells, whereas the loss of normal cell cycle control in the G_1 phase has been implicated in mammary tumor development and proliferation. Key targets of these pathways are specific sets of cyclin-cyclin-dependent kinase (CDK) protein complexes that function at specific stages of the cell cycle (34, 35). For example, many breast tumors show an aberrant expression and/or amplification of cyclin D1 or cyclin E, (36, 37), which both interact with G_1 phase CDKs. In fact, cyclin E expression has been shown to be the best diagnostic marker for breast cancer to date (38). CDK protein kinase activity is tightly regulated during passage through the cell cycle by the timely

* This study was supported by National Institutes of Health Public Health Service Grant CA102360 from the NCI, National Institutes of Health and by Grant 9WB-0148 awarded by the California Breast Cancer Research Program. The costs of publication of this article were defrayed in part by the payment of page charges. This article must therefore be hereby marked "*advertisement*" in accordance with 18 U.S.C. Section 1734 solely to indicate this fact.

§ Supported by Predoctoral Fellowship DAMD17-01-1-0175 awarded from the United States Department of Defense Breast Cancer Research Program.

‖ To whom correspondence should be addressed: Dept. of Molecular and Cell Biology, 591 LSA, The University of California at Berkeley, Berkeley, CA 94720-3200. Tel.: 510-642-8319; Fax: 510-643-6791; E-mail: glfire@berkeley.edu.

[1] The abbreviations used are: I3C, indole-3-carbinol; CDK, cyclin-dependent kinase; Rb, retinoblastoma; DIM, 3–3′-diindolylmethane; CDC, cell division cycle; GST, glutathione *S*-transferase; CAK, CDK-activating kinase; DTT, dithiothreitol; PMSF, phenylmethylsulfonyl fluoride; PBS, phosphate-buffered saline; Me_2SO, dimethyl sulfoxide.

appearance and degradation of cyclin-CDK protein complexes, CDK subunit phosphorylation, and interaction with a variety of CDK inhibitors (39). In early G_1, activation of CDK4-cyclin D and CDK6-cyclin D protein complexes initiate the phosphorylation of the retinoblastoma tumor suppressor protein (Rb), partially releasing the E2F family of transcription factors to permit the synthesis of cyclin E in mid to late G_1. CDK2 kinase activity increases as a result of its interaction with its regulatory partner, cyclin E, which directly hyperphosphorylates Rb, thereby further releasing the E2F transcription factors that in turn initiate the transcription of S phase genes. Although CDK2 and cyclin E have been shown to be dispensable for murine development (40, 41), these genes play a critical role in the transformation process of human breast cancer cells. For example, cyclin E-deficient cells have been shown to be resistant to oncogenic transformations (40) and overwhelming genetic, cellular, biochemical, and clinical evidence correlate aberrant cyclin E expression with tumorigenesis and poor patient prognosis, particularly in breast cancer (42–46). Thus, cyclin E-CDK2 protein complexes represents a critical potential target for anti-proliferative molecules, such as the natural indoles.

We have demonstrated that I3C directly induces a G_1 cell cycle arrest of human breast cancer cell lines through a pathway that is independent of estrogen receptor signaling and which targets specific G_1-acting cell cycle components (21). Our previous studies have shown that I3C down-regulates CDK6 transcription by disrupting the functional interactions of the Sp1 transcription factor with an Sp1-Ets composite DNA element in the CDK6 promoter (19). I3C also causes a pronounced decrease in CDK2 specific enzymatic activity and inhibited phosphorylation of endogenous Rb proteins (20), although the precise mechanism underlying this process has not been characterized. The activity, accessibility and cellular utilization of CDK2/cyclin E can be regulated at multiple levels, any one of which could be potentially targeted by I3C treatment. For example, in addition to cyclin association, the activation of CDK2 also requires the dephosphorylation of Thr^{14} and Tyr^{15} by Cdc25A (47) and an activating phosphorylation event at Thr^{160} by CDK-activating kinase (CAK) (48). Another mode of regulating CDK2 kinase activity is through the association with cyclin-dependent kinase inhibitors (CKI) such as p21, p27, and p57. Recent studies have also shown that the subcellular compartmentalization of either cyclin E or CDK2 greatly alters its enzymatic activity and accessibility to nuclear residing CAK, Cdc25A, and known substrates of CDK2 (49–51). In this study we demonstrate for the first time that I3C selectively controls the size distribution of the CDK2-cyclin E protein complex with concomitant alterations in cyclin E interactions and subcellular localization that results in an inhibition of CDK2 enzymatic activity in human breast cancer cells.

EXPERIMENTAL PROCEDURES

Materials—Dulbecco's modified Eagle's medium (DMEM), fetal bovine serum, calcium and magnesium-free PBS, L-glutamine, penicillin/streptomycin, and trypsin-EDTA were supplied by Cambrex/Biowhittaker (Walkersville, MD). I3C and DIM were purchased from LKT Laboratory Inc. (St. Paul, MN). [γ-^{32}P]ATP (3,000 Ci/mmol) was purchased from PerkinElmer Life Science Products. Insulin (bovine), tamoxifen, and tryptophol were purchased from Sigma.

Flow Cytometry Analysis of DNA Content—MCF-7 cells were plated at 30% confluency on 100-mm tissue culture plates and treated for the indicated time points with 100 μM I3C in complete media. An aliquot of harvested cells were hypotonically lysed in 0.5–1 ml of DNA staining solution (0.5 mg/ml propidium iodide, 0.1% sodium citrate, 0.05% Triton X-100). Cell debris was filtered and DNA content was analyzed as described previously (21).

Tissue Culture and Cell Lines—MCF-7 human breast cancer cell lines were grown in Dulbecco's modified Eagle's medium (DMEM) supplemented with 10% fetal bovine serum, 2 mM L-glutamine, 10 μg/ml insulin, 1.25 ml of 20,000 units/ml penicillin and streptomycin. Cells were maintained at subconfluency at 37 °C in humidified air containing 5% CO_2. I3C, DIM, tamoxifen, and tryptophol were dissolved in Me_2SO (99.9% high performance liquid chromatography grade; Aldrich) at concentrations 1000-fold higher than the final concentrations used.

Western Blot Analysis—After the indicated treatments, cells were lysed in either CDK2 lysis buffer (250 mM NaCl, 0.1% Triton X-100, 50 mM Tris/HCl, pH 7.3) or RIPA buffer (150 mM NaCl, 0.5% deoxycholate, 0.1% Nonidet P-40, 0.1% SDS, 50 mM Tris-HCl) containing protease and phosphatase inhibitors (50 μg/ml phenylmethylsulfonyl fluoride (PMSF), 10 μg/ml aprotinin, 5 μg/ml leupeptin, 0.1% sodium fluoride (NaF), 10 μg/ml β-glycerophosphate, and 0.1 mM sodium orthovanadate). Proteins were electronically transferred to nitrocellulose membranes (Micron Separations, Inc., Westboro, MA) and blocked as described previously (21). Blots were subsequently incubated at room temperature for an hour with anti-CDK2 (sc 748), CDK4 (sc260), and cyclin E1 (sc 198) antibodies. Blots probed with anti-p-Tyr (sc 7020), anti-p21(sc 398) or anti-p27 (sc 528) antibodies were either incubated at room temperature for 2–3 h or incubated overnight. All antibodies were used at a concentration of 1 μg/ml in TBST with the exception of anti-pTyr antibody, which was made in 1% nonfat dry milk/TBST. All antibodies were purchased from Santa Cruz Biotechnology (Santa Cruz, CA).

Immunoprecipitation and CDK2 Kinase Assays—After the indicated treatments, cells were lysed for 15 min at 4 °C in CDK2 lysis buffer with protease and phosphatase inhibitors (50 μg/ml PMSF, 10 μg/ml aprotinin, 5 μg/ml leupeptin, 0.1% sodium fluoride, 10 μg/ml β-glycerophosphate, and 0.1 mM sodium orthovanadate). Samples (500–800 μg of protein) were precleared as described previously (21) followed by incubation with 0.5 μg of anti-CDK2 or anti-cyclin E1 antibodies (Santa Cruz Biotechnology) for 2 h. Thirty microliters of a 1:1 bead slurry was added to each sample and left on a rocking platform for 30 min. The beads were washed with CDK2 lysis buffer and twice with kinase buffer (50 mM HEPES (pH 7.3), 5 mM $MnCl_2$, 10 mM $MgCl_2$) with protease and phosphatase inhibitors. Half of the immunoprecipitation was checked by Western blot analysis to confirm the efficiency of the immunoprecipitation. The remaining half of the immunoprecipitation was used to assess for kinase activity as described above.

I3C Directly Added to CDK2 IP/Kinase Assay—Immunoprecipitation of CDK2 was carried out as described above followed by a preincubation of the CDK2-immunoprecipitated protein complex with the indicated concentrations of I3C for 15 min at 30 °C. Half of the CDK2 immunoprecipitate was resolved on SDS-PAGE and Western blot analyzed for CDK2 while the remaining half was used to assess CDK2 kinase activity as described above. In a separate set of CDK2 immunoprecipitation, I3C was added concurrently with the [γ-^{32}P]ATP and histone H1 followed by a 15-min incubation at 30 °C and assayed for activity.

CDC25A Activity Assay—The constructs for GST-Cdc25A were a kind gift from Dr. Gregory Pierce's laboratory (Cancer Research Institute). Purified GST-Cdc25A was bacterially synthesized, sonicated in extraction buffer (1× PBS, 5 mM DTT, 10 mM Tris-HCl, pH 8), and the lysates were clarified by centrifugation. GST-Cdc25A fusion proteins were then absorbed onto glutathione-Sepharose beads, washed three times and eluted with 20 mM reduced glutathione. Cells were treated with either I3C or Me_2SO for 48 h followed by a CDK2 immunoprecipitation as described above. Half of the CDK2 immunoprecipitation was used for Western blot analysis while the remaining half was used for the Cdc25A kinase assay; CDK2 immune complexes were either incubated with 2 μg of purified GST-Cdc25A or GST-alone for 15 min at 30 °C in phosphate buffer (50 mM Tris, pH 8, 150 mM NaCl, 2 mM DTT, 2.5 mM EDTA). Half of the CDK2 immunoprecipitate was analyzed for CDK2 protein levels, and the remaining half was used to assess CDK2 kinase activity as described above.

Gel Filtration Column Chromatography—Gel filtration chromatography was carried out using a 50-cm length, 1.0-cm wide Kontes column (Fisher) packed with Superose 12 prep grade beads (Amersham Biosciences). Superose 12 beads were washed four times in column running buffer (250 mM NaCl, 0.1% Triton X-100, 50 mM Tris/HCl, pH 7.3) followed by degassing for 1 h via vacuum suction. The bead slurry was packed onto the Kontes column for 8 min at 2.3 ml/min and 55 min at 0.5 ml/min. Uniform packing was monitored using blue dextran (2000 kDa) followed by calibration of the column using the following molecular mass standards purchased from Amersham Biosciences: catalase (250 kDa), aldolase (158 kDa), albumin (67 kDa), and ovalbumin (45 kDa).

Cells were either treated with 100 μM I3C, 30 μM DIM, 1 μM tamoxifen, 100 μM tryptophol, or Me_2SO (control) for 48 h. Each sample was lysed in CDK2 lysis buffer with phosphatase and protease inhibitors

and cleared of cellular debris with by centrifugation at 15,000 × g. Cell lysates (800 μg) were then applied immediately onto a Kontes size exclusion column packed with Superose 12 beads and a total of 80 fractions were collected. Forty microliters of column lysate was taken for immunoblot analysis of CDK2 and 400 μl were precipitated (15 μl of 1 μg/ml bovine serum albumin, 1 ml of acetone, 400 μl of column lysate, mixed, and incubated at −70 for 3 h or overnight, followed by a 10 min spin at 15,000 × *g* at 4 °C), resuspended in 20 μl of 2× protein loading buffer used for immunoblotting for cyclin E and p21. For the column lysate immunoprecipitation/kinase assays, 2 consecutive gel filtration fractionations were conducted for each of the treatment groups. Column lysates were pooled, followed by the CDK2 immunoprecipitation/kinase assay described above.

Indirect Immunofluorescence—MCF-7 cells were plated on 8-well Lab-Tek Permanox slides (Nage Nunc International, Naperville, IL) at 20% confluency and treated for 48–72 h with either Me_2SO, I3C, DIM, tamoxifen or tryptophol (1 μl/ml of 1000× stock). Cells were washed with PBS, fixed with 3.7% formaldehyde, 0.01% glutaraldehyde for 15 min, and permeabilized with cold 50/50 acetone for 1 min. Cells were blocked for 5 min with PBS containing 4% goat serum (Jackson ImmunoResearch, West Grove, PA) followed by incubation with rabbit anti-CDK2 or mouse anti-cyclin E antibodies at a 1:150 dilution for 1.5 h (CDK2) at 25 °C or overnight for cyclin E at 4 °C. After five washes with cold PBS, cells were blocked and incubated with anti-rabbit rhodamine-texas red-conjugated secondary antibody (Jackson ImmunoResearch Laboratories, Inc.; diluted 1:300 in PBS) or anti-mouse FITC-conjugated secondary antibody (1:300) for 30 min. Cells were washed, mounted with clear nail polish and visualized on a Nikon Optiphot fluorescence microscope. Images were captured using Adobe Photoshop and a Sony DKC-5000 digital camera. Nonspecific fluorescence, as determined by incubation with secondary antibody alone was negligible.

Subcellular Fractionations—Cell pellets were resuspended at 5× volume in buffer A (0.01 M HEPES, pH 7.9, 1.5 mM $MgCl_2$, 0.01 M KCl, 0.5 mM DTT, 0.5 mM PMSF), incubated on ice for 30 min follow by a 5-min spin at 4 °C (1000 rpm). Cell pellets were resuspended at 2× volume in buffer A and dounced 100 strokes with type B pestle. Cells were checked with trypan blue to ensure at least 80% of cells were lysed, followed by a 20-min spin at 550 rpm. Supernatants were transferred to a new tube followed by 100,000 rpm centrifugation for 30 min in a ultracentrifuge to clear cytosolic extract of cellular debris. Nuclear pellets were resuspended in 1.5× cell volume with buffer B (20 mM HEPES, pH 7.4, 25% glycerol, 1.5 mM $MgCl_2$, 0.4 M NaCl, 0.2 mM EDTA. 0.5 mM DTT, 0.5 mM PMSF) and dounced 20 strokes with type B pestle. Extracts were nutated at 4 °C for 30 min followed by a 17,500 rpm centrifugation. The supernatants were dialyzed against 1000× volume of cold buffer C (0.02 M HEPES, pH 7.9, 5% glycerol, 1.5 mM $MgCl_2$, 0.1 M KCl, 0.2 mM EDTA, 0.5 mM DTT, 0.5 mM PMSF), followed by a 17,500 rpm centrifugation. Extracts were normalized and analyzed by Western blot.

Quantification of Autoradiography—Autoradiographic exposures were scanned with a UMAX UC630 scanner, and band intensities were quantified using the NIH Image program. Autoradiographs from a minimum of three independent experiments were scanned per time point.

RESULTS

Time Course of I3C Inhibition of CDK2 Kinase Activity and G_1 Cell Cycle Arrest—To determine the kinetics of the inhibition of CDK2 kinase activity by I3C, estrogen responsive human MCF-7 breast cancer cells were treated with or without 100 μM I3C over a 96-hour time course. This concentration of I3C was previously shown to be the optimal dose for the inhibition of cell growth without affecting cell viability (21). CDK2 protein complexes were immunoprecipitated from total cell lysates by using a CDK2-specific antibody, and half of each sample was assayed *in vitro* for kinase activity and the other half analyzed for CDK2 protein by Western blot analysis. CDK2 protein kinase activity was monitored by the ability of the immunoprecipitated CDK2-cyclin protein complexes to phosphorylate the C-terminal domain of Rb fused to GST. As shown in Fig. 1*A*, electrophoretic analysis of the phosphorylated GST-Rb showed that the I3C suppression of CDK2 kinase activity can be observed in cells treated as early as 24-h post-treatment, with near maximal inhibition observed by 72 h in I3C. A nonspecific IgG was used in one set of immunoprecipitations (*no IP lane*) as a negative control to demonstrate the specificity of the CDK2 kinase assay. A similar inhibition of CDK2 kinase activity was observed in estrogen receptor-negative breast cancer cells (data not shown). During the sample time course, the level of G_1 phase MCF-7 cells was examined by flow cytometry of propidium iodide-stained nuclei. As shown in Fig. 1*B*, I3C treatment induces a significant increase in the number of G_1 phase-arrested cells compared with untreated cells, which correlates closely to the kinetics of I3C inhibition of CDK2 enzymatic activity.

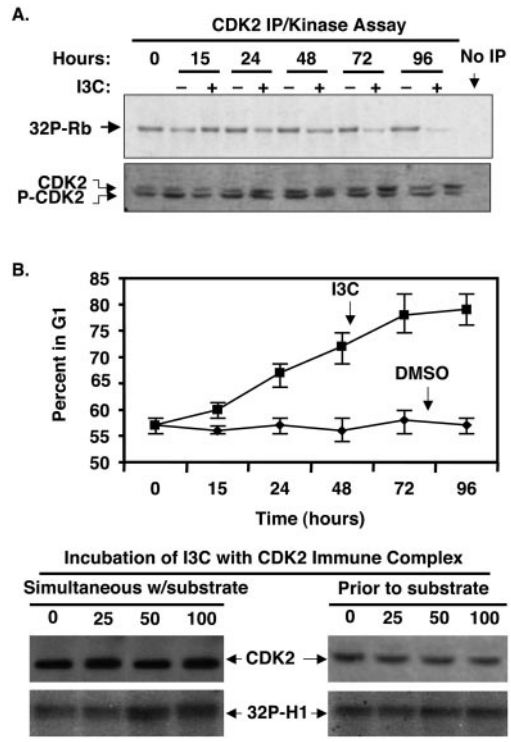

FIG. 1. **I3C inhibits CDK2 kinase activity in MCF-7 breast cancer cells but does not act as a direct enzymatic inhibitor.** MCF-7 cells were treated with or without 100 μM I3C for the indicated time points followed by a CDK2 immunoprecipitation (*IP*). *A*, half of each immunoprecipitate was used to assess CDK2 kinase activity using GST-Rb as a substrate (*top panel*). The remaining half of each immunoprecipitate was Western blot analyzed for CDK2 protein (*bottom panel*). *B*, flow cytometry was employed to determine the percentage of cells in the G_1 phase of the cell cycle under I3C-treated or untreated conditions. Data are the mean of three experiments, and the bars represents S.E. *C*, indicated concentrations of I3C were added to CDK2 immunoprecipitated protein complexes either simultaneously with or 15 min prior to the addition of [^{32}P]ATP and the histone H1 substrate. Each immunoprecipitate was assayed for CDK2 kinase activity (*bottom panels*) and protein level Western blot analyses of CDK2 (*top panels*).

Given the chemical nature of I3C, it is conceivable that this indole could act as a direct enzymatic inhibitor of CDK2, and thereby prevents the CAK phosphorylation of CDK2. To examine this possibility, a range of I3C concentrations was added to individual CDK2 immunoprecipitates either prior to or simultaneous with the addition of the histone H1 substrate and [γ-^{32}P]ATP. As shown in Fig. 1*C*, I3C has no significant effect on the *in vitro* CDK2 kinase activity. These results demonstrate that I3C does not inhibit CDK2 kinase activity through direct interactions with the CDK2 protein immunocomplex.

Western blot analyses of CDK2 immunoprecipitates show that I3C treatment did not alter the total level of CDK2 protein (Fig. 1*A*), indicating that I3C inhibits total cellular CDK2 specific enzymatic activity. CDK2 protein migrates as a doublet, and the faster migrating CDK2 band represents the CAK-phosphorylated Thr^{160} form of CDK2, which is necessary for enzymatic activity (48). The Western blots also revealed that in

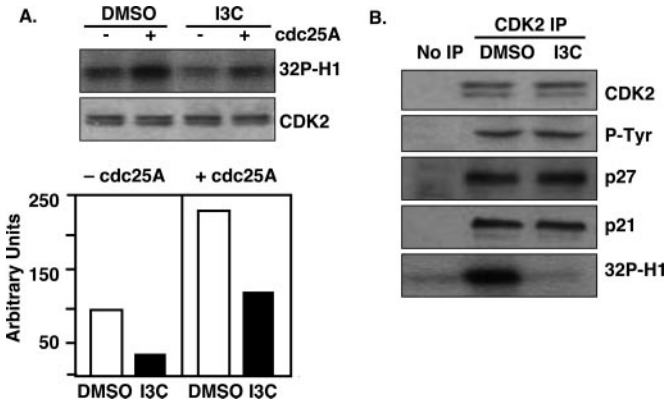

FIG. 2. **Effects of I3C on CDK2 phosphorylation and interaction with small molecule inhibitors.** *A*, CDK2 protein complex was isolated by immunoprecipitation from I3C-treated and untreated cells. Each immunoprecipitate was incubated with either 2 μg of purified GST-Cdc25A or GST alone followed by an *in vitro* kinase assay (*upper panel*). Half of each immunoprecipitate were analyzed for CDK2 protein levels (*lower panel*). The bar graph represents the quantification of the level of CDK2 kinase specific activity observed in the presence or absence of Cdc25A. *B*, CDK2 immune complexes from I3C-treated and untreated cells were Western blot analyzed for the indicated protein: CDK2, phosphotyrosine (*p-Tyr*) phosphorylated CDK2, p21, and p27. The other half of the immunoprecipitate was assayed for kinase activity (*lower gel*).

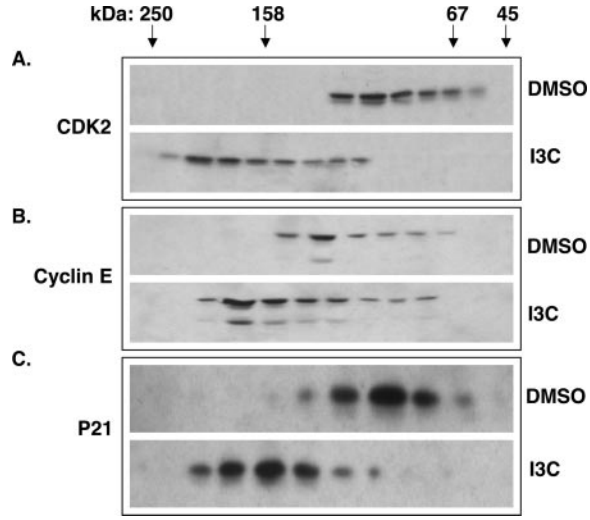

FIG. 3. **I3C alters the size distribution of the CDK2 protein complex.** MCF-7 cells were treated with or without 100 μM I3C for 48 h, and total cell lysates were fractionated by a size exclusion column as described under "Experimental Procedures." Column fractions were analyzed by Western blotting for the presence of CDK2 (*A*), cyclin E (*B*), and p21 (*C*). Catalase (250 kDa), aldolase (158 kDa), albumin (67 kDa), and ovalbumin (45 kDa) were the molecular mass standards used to calibrate the column.

MCF-7 breast cancer cells, the CAK phosphorylated form of CDK2 is modestly reduced in samples immunoprecipitated from the 72 and 96 h I3C-treated cells, but not at early time points. These results suggest that the events leading to the inhibition of CDK2 kinase activity by I3C precedes the decrease in the CAK phosphorylation of CDK2 protein.

I3C Does Not Affect the Inhibitory Phosphorylation of CDK2 or Levels of Known CDK2 Inhibitors That Associate with the CDK2 Protein Complex—To address whether I3C had an effect on the inhibitory phosphorylation events, CDK2 immune complexes from control or I3C-treated cells were first treated with either recombinant GST-alone or GST-Cdc25A and the kinase activity of the CDK2 immunocomplexes assayed *in vitro* using histone H1 as a substrate. As shown in Fig. 2*A*, exposure to active Cdc25A caused the same approximate 2-fold increase in CDK2 specific enzymatic activity in the immune complexes isolated from control and I3C-treated cells. Importantly, after Cdc25A treatment, the enzymatic activity of the CDK2 complexes immunoprecipitated from I3C-treated cells remained significantly reduced compared with the control samples. Thus, the I3C inactivation of the CDK2 enzymatic activity was most likely not caused by an increase in the negative phosphorylation events on residues Thr^{14}/Tyr^{15} on CDK2. This was confirmed by Western blot analysis of Tyr-phosphorylated forms of CDK2 in a CDK2 complex immunoprecipitated from I3C-treated or untreated cells. As shown in Fig. 2*B*, I3C had no effect on the presence of the Tyr^{14}-phosphorylated forms of CDK2.

To address other canonical mechanisms of regulating CDK2 kinase activity, the presence of known CDK inhibitors associated with the CDK2 protein complex in I3C-treated or untreated cells were analyzed by co-immunoprecipitation. MCF-7 human breast cancer cells were treated with either Me_2SO or I3C for 48 h followed by a CDK2 immunoprecipitation and Western blot analysis of p21 and p27. As shown in Fig. 2*B*, the level of p21 and p27 associated with CDK2 did not change with I3C treatment despite drastic reductions in kinase activity as measured by the phosphorylation of histone H1 (Fig. 2*B*, *lower panel*). No detectable p57 was observed in the CDK2 immunoprecipitates from these cells (data not shown). The cyclin E associated with the CDK2 protein complex is characterized later in this study. We conclude that the I3C-induced inhibition of CDK2 kinase activity is not due to an increase in association with known CDK2 inhibitors or changes in inhibitory phosphorylation states of CDK2.

I3C Alters the Size Distribution of the CDK2 Protein Complex—As a first approach to determine if I3C alters the composition of the CDK2 protein complex, the sizes of the CDK2 protein complexes produced in breast cancer cells treated with or without I3C were biochemically characterized. Equal amounts of total cell lysates (800 μg) were fractionated on a Sepharose size exclusion gel filtration column. Individual gel filtration fractions were electrophoretically separated by SDS-PAGE, followed by Western blot analysis of CDK2, cyclin E, and p21. As shown in Fig. 3*A* (*upper panel*), in proliferating MCF7 breast cancer cells, the CDK2 protein complex eluted with a native size of ~90 kDa. Strikingly, in I3C growth-arrested cells, CDK2 eluted as part of a much larger 180–200 kDa protein complex (Fig. 3*A*, *lower panel*). Analysis of the fractionation profile of cyclin E and p21 (Fig. 3, *B* and *C*), showed a similar result.

CDK2 Kinase Activity Is Associated Primarily with the 90 kDa CDK2 Protein Complex—To determine the CDK2 enzymatic activity in each of the CDK2 protein complexes, individual fractions from the gel filtration columns were immunoprecipitated with CDK2 antibodies, and the kinase activity of the immune complexes were monitored *in vitro*. As shown in Fig. 4*A*, most of CDK2 protein kinase activity is associated with the 90 kDa protein complex, as assayed by the *in vitro* phosphorylation of histone H1. Despite an abundant amount of CDK2 protein in the 200 kDa protein complex formed in I3C-treated cells, the majority of the kinase activity was observed in fractions that correspond to the 90 kDa CDK2 protein complex (Fig. 4*B*). Consistent with the overall change in the fractionation of the CDK2 protein complex, I3C-treated cells produce a significantly reduced level of the enzymatically active 90 kDa CDK2 protein complex compared with the same fractions from control cells. These results demonstrate that I3C induces the formation of a larger (200 kDa) CDK2 complex that is enzymatically inactive. Interestingly, cyclin E association with CDK2 in the column lysates changed significantly with I3C

treatment in that the 50 kDa cyclin E form is more abundant in the inactive, 200 kDa CDk2 protein complex observed with I3C treatment as compared with control. Furthermore, a 75 kDa cyclin E immunoreactive protein co-precipitated with CDK2 in fractions that correspond to the 200 kDa protein complex, suggesting that it can partially account for the 100 kDa shift in size of the CDK2 protein complex.

I3C Alters the Cyclin E Form That Associate with the Larger CDK2 Protein Complex—Different forms of cyclin E can associate with CDK2 and confer different levels of CDK2 enzymatic activity. Several lower molecular weight cyclin E forms are found in breast cancer tissues and are associated with higher CDK2 enzymatic activity (52). In contrast, the larger form of cyclin E (50 kDa) is found in both normal and tumorigenic tissues, and are associated with CDK2 protein complexes that display a reduced enzymatic activity as compared with the smaller forms of cyclin E (52). Co-immunoprecipitation was used to examine the nature of the cyclin E forms that associate with CDK2 protein complexes in growing and I3C growth-arrested breast cancer cells. As shown in Fig. 5, the 35 kDa lower molecular mass form of cyclin E associated with the active CDK2 protein complex in untreated cells is drastically reduced after I3C treatment. Correspondingly, there is a significant increase in the level of both a 50 kDa form and an unusual 75 kDa cyclin E immunoreactive protein that is associated with the inactive CDK2 protein complex detected in I3C-treated cells. The precise function of this 75 kDa protein is not known, although because it is specifically recognized by cyclin E antibodies and binds to CDK2, we propose that it likely functions as a regulator of CDK2. In whole cell extracts, I3C has no effect on the total cellular level of this 75 kDa cyclin E immunoreactive protein (data not shown), suggesting that I3C stimulates the association of the CDK2 protein complex with this 75 kDa cyclin E immunoreactive protein. We propose that the increase in CDK2 association with the 50 kDa cyclin E and the 75 kDa cyclin E immunoreactive protein likely accounts for the approximate 100 kDa increase in size of the CDK2 protein complex observed in I3C-treated cells (Fig. 4). CDK2 kinase activity was assessed within the CDK2 immunoprecipitates from control or I3C-treated cells using histone H1 as the substrate. As shown in the *bottom panel* of Fig. 5*A*, the CDK2-associated kinase activity was significantly reduced in samples isolated from I3C-treated cells, which contained elevated levels of the 50 cyclin E and 75 kDa cyclin E immunoreactive protein associated with the CDK2 protein complex.

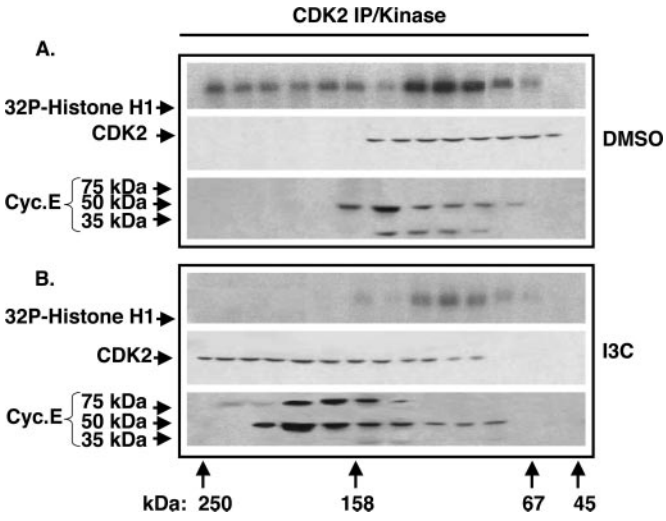

FIG. 4. **CDK2 kinase activity is associated with the 90 kDa CDK2 protein complex.** MCF-7 cells were treated with (*B*) or without (*A*) 100 μM I3C, and total cell lysates were fractionated by a size exclusion column as described under "Experimental Procedures." CDK2 was immunoprecipitated from column lysates, and assayed for CDK2 protein kinase activity (*top gels* in each set) or for the presence of CDK2 or cyclin E protein by Western blot analysis (*bottom gels* in each set).

The anti-tumorigenic effects of I3C *in vivo* are partly due to the formation of DIM, which is a natural dimerization product of I3C in acidic conditions (12). DIM has been shown to inhibit MCF-7 breast cancer cell growth and down-regulate CDK2 kinase activity through the transcriptional induction of the p21 CDK inhibitor (53). Furthermore, because of the fact that a fraction of I3C is converted into DIM in breast cancer cells (54), it is critical to evaluate whether the observed changes in the 50 kDa cyclin E and 75 kDa cyclin E immunoreactive protein that associate with CDK2 protein complexes are specific for the I3C signaling pathway, or a general effect of growth inhibition by indoles. Under conditions in which I3C and DIM induce a parallel G_1 cell cycle arrest as monitored by their similar flow cytometry profiles (Fig. 5*B*), DIM did not alter the association of the different cyclin E forms with CDK2 as compared with control (Fig. 5*A*, *DMSO versus DIM*) despite a drastic reduction in CDK2 kinase activity. These results suggest that the association of the higher molecular mass forms of cyclin E with the CDK2 protein complex is an I3C-specific indole response.

The Formation of the 200 kDa CDK2 Protein Complex Is an I3C-specific Response—To test whether the change in size distribution of the CDK2 protein complex is specific to the I3C

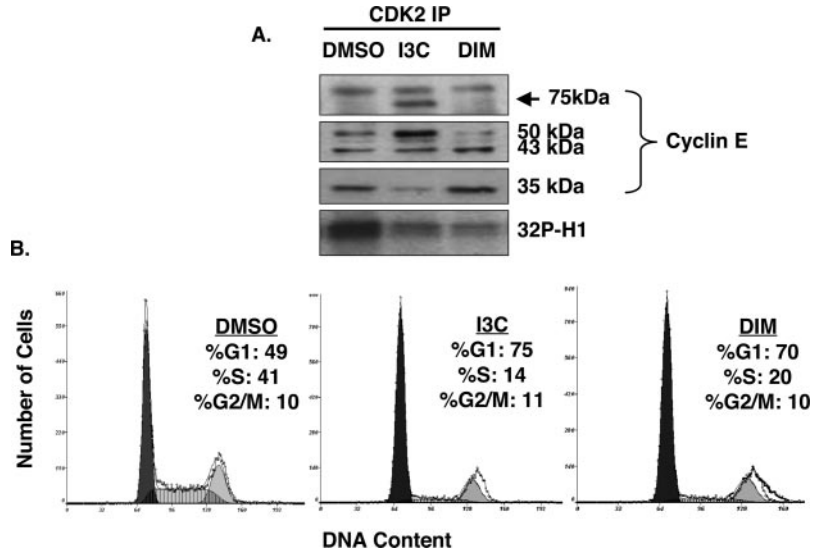

FIG. 5. **Effects of I3C on the associated cyclin E forms with the CDK2 protein complex.** *A*, CDK2 was immunoprecipitated from MCF-7 cells treated for 72 h with either Me_2SO (*DMSO*), 100 μM I3C, or 30 μM DIM. Each set of immunoprecipitated CDK2 protein complex was either fractionated by SDS-PAGE and Western blot analysis for cyclin E (*top three panels*), or was assayed for CDK2 kinase activity using histone H1 as a substrate (^{32}P-H1). *B*, flow cytometry analysis of cells that were treated with either Me_2SO, I3C, or DIM for 72 h as described under "Experimental Procedures."

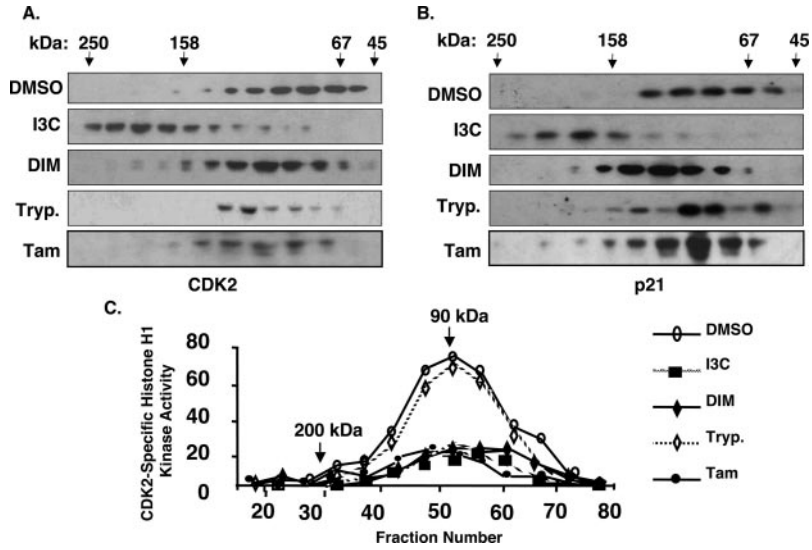

FIG. 6. **Formation of the 200 kDa CDK2 protein complex is specific to the I3C response.** Cells were treated with 100 μM I3C, 30 μM DIM, 100 μM tryptophol (*Tryp.*), or 1 μM tamoxifen (*Tam*), or were incubated with the Me_2SO (*DMSO*) vehicle control for 48 h. Cell lysates were fractionated from gel filtration chromatography as described under "Experimental Procedures," and column fractions analyzed for the presence of either CDK2 (*A*) or p21 (*B*) by Western blot analysis. A third set of immunoprecipitated CDK2 protein complex from the fractionated cell lysates was assayed for CDK2 kinase activity as described in Fig. 4, and the level of phosphorylated histone H1 quantified by phosphorimaging (*C*).

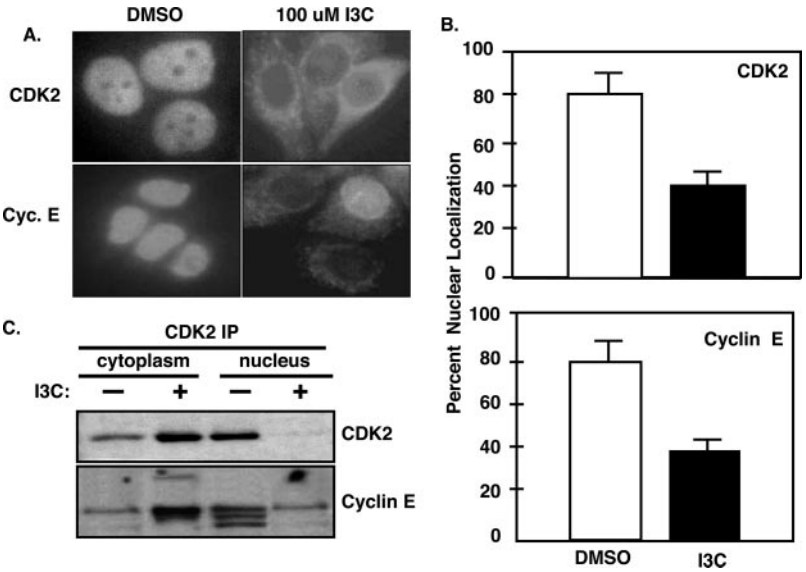

FIG. 7. **Effects of I3C on the subcellular localization of CDK2 and cyclin E.** *A*, MCF-7 cells were treated with or without 100 μM I3C for 48 h followed by indirect immunofluorescence using CDK2- or cyclin E-specific antibodies. *B*, percentage of cells containing nuclear residing CDK2 protein (*top graph*) or cyclin E protein (*bottom graph*) was quantified by evaluating ~1000 random cells (*C*) I3C-treated and untreated cells were biochemically fractionated into nuclear and cytoplasmic fractions by differential centrifugation. CDK2 was isolated via an immunoprecipitation and resolved by SDS-PAGE and Western blot analyzed for CDK2 and cyclin E.

response, breast cancer cells were treated for 48 h with several agents known to induce a G_1 cell cycle arrest; 100 μM I3C, 30 μM DIM, or 1 μM of the estrogen antagonist, tamoxifen. Control cells were either treated with 100 μM tryptophol, an indole with a structure similar to I3C but does not exhibit any anti-proliferative properties (19), or with the Me_2SO vehicle control. Total cell extracts were fractionated by gel filtration chromatography and individual fractions were Western blot analyzed for either CDK2 or p21 protein. As shown in Fig. 6, under conditions in which I3C treatment caused a 100 kDa shift in size of the CDK2 protein complex, tamoxifen, DIM, or tryptophol did not significantly alter the size distribution of CDK2. Additionally, close inspection of the results revealed that the CDK2 protein complex is slightly larger in DIM and tamoxifen-treated cells compared with the vehicle control cells (Fig. 6, *A* and *B*). Treatment with DIM or tamoxifen induced a significant increase in the level of CDK2 protein complex-associated p21 (Fig. 6*B*), which likely accounts for this small increase in the overall size of the CDK2 protein complex. This result is consistent with previous studies showing that tamoxifen and DIM treatments increase the level of p21 associated with the CDK2 complex, thus rendering it inactive (55, 56).

To determine the distribution of CDK2 enzymatic activity, CDK2-immunoprecipitated protein complex from column fractions were assayed *in vitro* using histone H1 as a substrate. As shown in Fig. 6*C*, CDK2 kinase activity is significantly reduced in I3C, DIM, and tamoxifen-treated cells compared with control cells (Me_2SO or tryptophol). The majority of CDK2 kinase activity fractionated as a 90 kDa CDK2 protein complex. The reduced level of CDK2 enzymatic activity after I3C treatment is likely due to the formation of the larger 200 kDa inactive complex, whereas, in DIM or tamoxifen-treated cells, the reduction in CDK2 kinase activity correlated with the increase in p21 observed in fractions that correspond to the distribution of CDK2. These results also show that I3C acts through a pathway that is distinct from either DIM or tamoxifen in regulating CDK2 enzymatic activity.

I3C Alters the Subcellular Localization of CDK2 and Cyclin—Subcellular compartmentalization of CDKs and their regulatory cyclins play a critical role in controlling their activity and cell cycle progression (57). Several studies have shown that the localization of CDK2 is highly dependent on cyclin association (51, 58, 59). We therefore tested whether I3C treatment had an effect on cyclin E and CDK2 localization using indirect immunofluorescence microscopy. Cells were treated with either Me_2SO or 100 μM I3C for 48 h, permeabilized and incubated with either CDK2 or cyclin E primary antibodies, followed by the appropriate secondary antibodies. Typical immunofluorescence staining is shown in Fig. 7*A* where CDK2 and cyclin E are localized to the nucleus in control cells and is redistributed

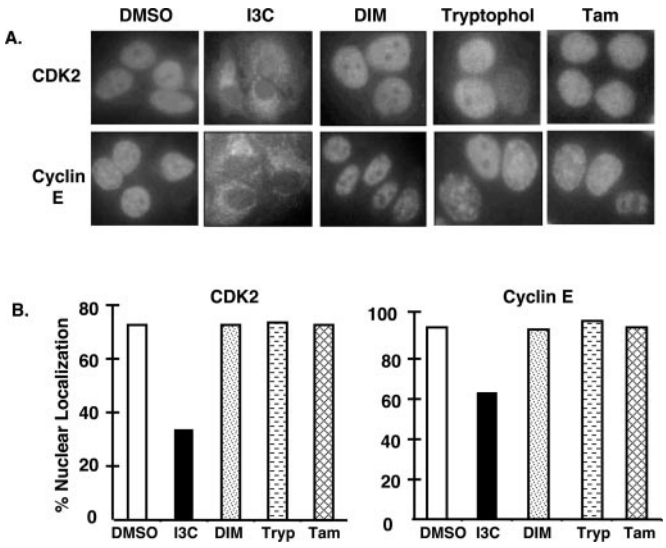

FIG. 8. **I3C-specific changes in subcellular localization of CDK2 and cyclin E.** MCF-7 cells were treated with 100 μM I3C, 30 μM DIM, 100 μM tryptophol, or 1 μM tamoxifen (*Tam*), or were incubated with the Me_2SO (*DMSO*) vehicle control for 48 h. *A*, subcellular localization of either CDK2 or cyclin E was analyzed by indirect immunofluorescence. *B*, percentage of cells containing nuclear residing CDK2 or cyclin E was quantified for each treatment group.

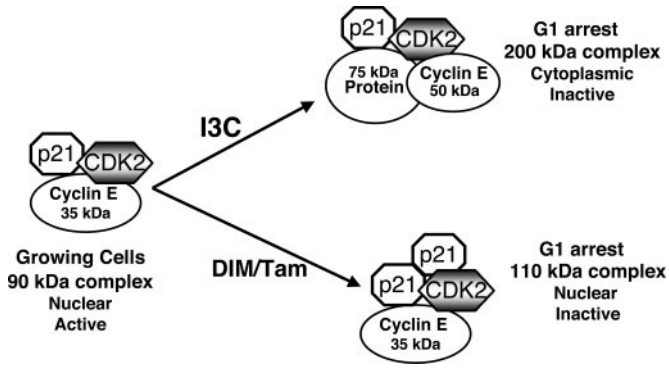

FIG. 9. **Summary of the differential regulation of CDK2 protein complex by I3C, DIM, and tamoxifen in breast cancer cells.** In proliferating cells, CDK2 protein complexes are ~90 kDa in size, contain higher levels of the 35 kDa cyclin E, and reside predominantly in the nucleus in an enzymatically active state. I3C treatment induces a G_1 cell cycle arrest and causes the formation of a significantly larger 200 kDa CDK2 protein complex that contains a 50 kDa cyclin E and a 75 kDa cyclin E immunoreactive protein. This I3C induced 200 kDa CDK2 protein complex is enzymatically inactive, localizes to the cytoplasm, and displays no apparent change in the level of associated p21. Treatment with DIM or tamoxifen induces a G_1 cell cycle arrest of MCF-7 breast cancer cells; however, in contrast to I3C, neither agent has an affect on the associated forms of cyclin E with the CDK2 protein complex or its subcellular localization. Treatment with DIM or tamoxifen causes the formation of an inactive 110 kDa CDK2 protein complex that is because of the increased association of CDK inhibitors (p21) with CDK2.

to the cytoplasm with I3C treatment. Individual cells in each population were counted, and the number of cells containing nuclear staining of cyclin E or CDK2 *versus* the total number of cells present were assessed and statistically analyzed using the Student's *t* test. Under proliferative conditions (Me_2SO-treated), ~80% of the cells contained nuclear staining for CDK2. In contrast, I3C treatment caused a significant increase in the level CDK2 and cyclin E that were localized to the cytoplasm. An average of three independent experiments showed that there was a 40% reduction in the level of nuclear CDK2 and cyclin E in I3C-treated human breast cancer cells as compared with control cells (Fig. 7*B*).

In conjunction with the immunofluorescence studies, the subcellular fractionation of CDK2 and cyclin E was examined by Western blot analysis of cytoplasmic and nuclear fractions from I3C-treated and untreated cells. As shown in Fig. 7*C*, I3C treatment significantly increased the level of CDK2 and the CDK2-associated, 50 kDa cyclin E and the 75 kDa cyclin E immunoreactive protein in the cytoplasmic fractions with a corresponding decrease in their protein levels in the nuclear fractions as compared with control cells.

To further establish the I3C specificity of the redistribution of CDK2 and cyclin E localization, indirect immunofluorescence was used to examine the subcellular distribution of both proteins in cells treated with I3C, DIM, tamoxifen, tryptophol, or the Me_2SO vehicle control. As shown in Fig. 8*A*, under conditions where I3C increases the level of cytoplasmic CDK2 and cyclin E subcellular localization, DIM, or tamoxifen have no effect on the subcellular localization of CDK2 or cyclin E compared with the controls sets of cells (tryptophol or vehicle control-treated cells). Fig. 8*B* shows a 40% reduction in the number of cells containing nuclear localization of both cyclin E and CDK2 with I3C treatment as compared with control cells, and no change was observed in the localization profile of cyclin E or CDK2 among cells that were treated with tamoxifen or DIM. As expected, tryptophol-treated cells were indistinguishable from the vehicle control-treated cells. Taken together, these results demonstrate that that the change in subcellular localization and the increase in the size of the CDK2 protein complex are specific to the I3C growth inhibitory response.

DISCUSSION

I3C is a promising chemotherapeutic agent for treatment of human breast cancer, and other reproductive cancers, because of its potent growth inhibitory properties (18–23, 60–62), and repression of invasion and migration of cultured breast cancer cell lines (24). Elucidation of the molecular mechanisms and cell cycle targets of the I3C anti-proliferative signaling pathway provides critical information that could potentially be exploited in the development of novel indole-based therapeutic strategies. We previously documented that I3C induces a G_1 cell cycle arrest of human breast cancer cells that is accompanied by the dual inhibition CDK6 and CDK2 kinase activities (19). I3C and its natural dimerization product DIM (12) have been shown to inhibit CDK2 enzymatic activity, although the distinction in the mechanisms underlying the effects of these two indoles was unknown. We now establish a new and unique feature of the I3C signaling pathway by establishing that I3C induces a robust down-regulation of CDK2 kinase activity that is accompanied by selective alterations in the cyclin E composition, size distribution and subcellular localization of the CDK2 protein complex. Furthermore, we show that this mechanism of regulating CDK2 function is specific to the I3C anti-proliferative signaling pathway that is distinguishable from the actions of DIM and the anti-estrogen tamoxifen.

As summarized in Fig. 9, in growing breast cancer cells, a 90 kDa CDK2 protein complex that is enzymatically active resides in the nucleus, and includes both the p21 CDK inhibitor and the 35 kDa lower molecular mass form of cyclin E. After I3C treatment, a 200 kDa CDK2 protein complex is formed that is enzymatically inactive and is localized mostly to the cytoplasm. This larger CDK2 protein complex was shown to contain elevated levels of the 50 kDa form of cyclin E and a unique 75 kDa cyclin E immunoreactive protein, but not the lower molecular mass cyclin E form observed in proliferating cells. The striking increase in size of the CDK2 protein complex detected in I3C-treated cells has never been observed in other cell systems.

Treatment of MCF-7 human breast cancer cells with either DIM or the anti-estrogen tamoxifen induces a G_1 cell cycle

arrest and inhibits CDK2 enzymatic activity (20, 53). In contrast to the effects of I3C, DIM or tamoxifen did not alter the interaction of the lower molecular mass forms of cyclin E with the CDK2 protein complex or regulate the nuclear localization of the CDK2 protein complex (summarized in Fig. 9). Thus, the formation of the larger CDK2 protein complex observed in I3C-treated cells is not an indirect consequence of the cells undergoing a G_1 cell cycle arrest. A key problem in using tamoxifen in the clinical management of breast cancer is that a majority of the cancers that do respond to this anti-estrogen eventually acquire resistance to prolong tamoxifen treatment (63). We propose that the previously reported synergistic inhibition of CDK2 kinase activity by combinatorial treatments with I3C and tamoxifen (20) is due to ability of these two anti-cancer agents to disrupt CDK2 function through different cellular pathways. Because lower doses of tamoxifen could potentially be used in the presence of I3C, conceivably this indole could potentially be used to overcome the tamoxifen resistance or prolong the duration in which tamoxifen is effective in suppressing the growth of breast cancer cells. Similarly, of I3C and DIM combinatorial regiments could also be developed for treating breast cancer.

A novel feature of our results is that I3C selectively increases the size of the CDK2 protein complex, from 90 to 200 kDa, that we propose is due to the association of the higher molecular mass 50 kDa cyclin E and 75 kDa cyclin E immunoreactive protein that associate with CDK2. In growing cells not treated with I3C, the 90 kDa CDK2 protein complex contains the 35 kDa lower molecular mass form of cyclin E. The discovery that the lower molecular mass cyclin E forms reside in the nucleus and associate with enzymatically active CDK2 compared with the 50 kDa cyclin E form suggests a specific role of cyclin E in regulating CDK2 function. In this regard, tumorigenic tissues from aggressive breast tumors express elevated levels of the lower molecular weight forms of cyclin E as compared with normal breast epithelium (52, 64, 65). Based on this newly appreciated level of regulating CDK2 kinase activity by cyclin E, we propose that the inhibition CDK2 kinase activity by I3C is due to the replacement of the lower molecular mass forms of cyclin E with the 50 kDa form and the 75 kDa cyclin E immunoreactive protein (summarized in Fig. 9). Consistent with this concept, enzymatic activity of the 200 kDa CDK2 protein complex formed after I3C treatment is significantly reduced compared with the high enzymatic activity of the 90 kDa CDK2 protein complex detected in breast cancer cells not treated with I3C. Studies are underway to functionally characterize the precise roles of the 50 kDa cyclin E and 75 kDa cyclin E immunoreactive protein in controlling CDK2 kinase activity and mediating the G_1 cell cycle arrest.

Our results also eliminated several established modes of regulating CDK2 kinase activity by I3C. The direct addition of I3C to CDK2 immunoprecipitates demonstrated that I3C does not act as a small molecule enzymatic inhibitor of CDK2 kinase activity. We also eliminated the possibility that I3C could be changing the phosphorylation states of CDK2 or the level of known CDK inhibitors (p21 and p27) that associate with the CDK2 protein complex. Although the inhibitory phosphorylation events are unaffected by I3C treatment, the level of CAK-phosphorylated CDK2 is modestly reduced with prolonged I3C treatment. This effect could be because of the decreased association of the 35 kDa cyclin E, which has been shown to induce CAK phosphorylation of CDK2 (66). Because the down-regulation of CDK2 kinase activity by I3C preceded the reduction in the level of CAK phosphorylation of CDK2, it is unlikely that the primary mechanism by which I3C regulates CDK2 kinase activity occurs through CAK.

The redistribution of the CDK2 protein complex to the cytoplasm in I3C-treated cells represents an effective mode of growth regulation because it prevents access to a variety of substrates and regulatory proteins. For example, key regulators of CDK2 (Cdc25A and CAK), as well as its key substrates (Rb, NPAT, BRCA1, and Cdc6), which play key roles in initiating S-phase transition, reside in the nucleus. Nucleocytoplasmic shuttling of CDK and cyclin E has been shown to be dynamically regulated, and the steady state accumulation of nuclear CDK2/cyclin E is caused by a faster rate of nuclear import as compared with the rate of nuclear export (67). This process can be regulated by several extracellular signals in other systems. For example, TGF-β and vitamin D induce the cytoplasmic localization of CDK2 leading to a decrease in Rb phosphorylation and a G_1 cell cycle arrest (16, 51). I3C treatment increases the steady state cytoplasmic localization of both CDK2 and cyclin E, and it is therefore conceivable that I3C could either reduce the rate of nuclear import of CDK2-cyclin E protein complexes or increase the rate of nuclear export. Recent studies show that CDK2 localization is controlled by its association with cyclin E (58, 59). Therefore it is tempting to consider that association of the higher molecular weight forms of cyclin E with CDK2, in particular the 75 kDa cyclin immunoreactive protein, under I3C-treated conditions, could sequester the CDK2-cyclin E protein complex in the cytoplasm. For example, replacement of the lower molecular mass cyclin E form with the higher molecular mass forms of cyclin E could potentially mask a critical nuclear localization signal or activate a nuclear export signal. Further studies are needed to determine the precise mechanistic relationship between the increase in size distribution of the CDK2 protein complex, and the I3C control of nucleocytoplasmic shuttling of the CDK2 protein complex with the overall G_1 cell cycle arrest.

Acknowledgments—We thank Christine Brew, Jocelyn Hsu, and Erin J. Cram for helpful discussions and critical comments during the course of our study.

REFERENCES

1. Birt, D. F., Pelling, J. C., Nair, S., and Lepley, D. (1996) *Prog. Clin. Biol. Res.* **395,** 223–234
2. Lopez-Otin, C., and Diamandis, E. P. (1998) *Endocr. Rev.* **19,** 365–396
3. Bresnick, E., Birt, D. F., Wolterman, K., Wheeler, M., and Markin, R. S. (1990) *Carcinogenesis* **11,** 1159–1163
4. Loub, W. D., Wattenberg, L. W., and Davis, D. W. (1975) *J. Natl. Cancer Inst.* **54,** 985–988
5. Grubbs, C. J., Steele, V. E., Casebolt, T., Juliana, M. M., Eto, I., Whitaker, L. M., Dragnev, K. H., Kelloff, G. J., and Lubet, R. L. (1995) *Anticancer Res.* **15,** 709–716
6. Wattenberg, L. W., and Loub, W. D. (1978) *Cancer Res.* **38,** 1410–1413
7. Morse, M. A., LaGreca, S. D., Amin, S. G., and Chung, F. L. (1990) *Cancer Res.* **50,** 2613–2617
8. Bradlow, H. L., Michnovicz, J., Telang, N. T., and Osborne, M. P. (1991) *Carcinogenesis* **12,** 1571–1574
9. Scholar, E. M., Wolterman, K., Birt, D. F., and Bresnick, E. (1989) *Nutr. Cancer* **12,** 121–126
10. Sharma, S., Stutzman, J. D., Kelloff, G. J., and Steele, V. E. (1994) *Cancer Res.* **54,** 5848–5855
11. Bradfield, C. A., and Bjeldanes, L. F. (1984) *Food Chem. Toxicol.* **22,** 977–982
12. Bradfield, C. A., and Bjeldanes, L. F. (1987) *J. Toxicol. Environ. Health* **21,** 311–323
13. Chen, I., McDougal, A., Wang, F., and Safe, S. (1998) *Carcinogenesis* **19,** 1631–1639
14. Liu, H., Wormke, M., Safe, S. H., and Bjeldanes, L. F. (1994) *J. Natl. Cancer Inst.* **86,** 1758–1765
15. Michnovicz, J. J., and Bradlow, H. L. (1990) *J. Natl. Cancer Inst.* **82,** 947–949
16. Yang, E. S., and Burnstein, K. L. (2003) *J. Biol. Chem.* **278,** 46862–46868
17. Srivastava, B., and Shukla, Y. (1998) *Cancer Lett.* **134,** 91–95
18. Firestone, G. L., and Bjeldanes, L. F. (2003) *J. Nutr.* **133,** 2448S-2455S
19. Cram, E. J., Liu, B. D., Bjeldanes, L. F., and Firestone, G. L. (2001) *J. Biol. Chem.* **276,** 22332–22340
20. Cover, C. M., Hsieh, S. J., Cram, E. J., Hong, C., Riby, J. E., Bjeldanes, L. F., and Firestone, G. L. (1999) *Cancer Res.* **59,** 1244–1251
21. Cover, C. M., Hsieh, S. J., Tran, S. H., Hallden, G., Kim, G. S., Bjeldanes, L. F., and Firestone, G. L. (1998) *J. Biol. Chem.* **273,** 3838–3847
22. Zhang, J., Hsu, B. A. J., Kinseth, B. A. M., Bjeldanes, L. F., and Firestone, G. L. (2003) *Cancer* **98,** 2511–2520
23. Chatterji, U., Riby, J. E., Taniguchi, T., Bjeldanes, E. L., Bjeldanes, L. F., and Firestone, G. L. (2004) *Carcinogenesis* **25,** 1119–1128

24. Meng, Q., Goldberg, I. D., Rosen, E. M., and Fan, S. (2000) *Breast Cancer Res. Treat.* **63,** 147–152
25. Meng, Q., Qi, M., Chen, D. Z., Yuan, R., Goldberg, I. D., Rosen, E. M., Auborn, K., and Fan, S. (2000) *J. Mol. Med.* **78,** 155–165
26. Chen, Y. H., Riby, J., Srivastava, P., Bartholomew, J., Denison, M., and Bjeldanes, L. (1995) *J. Biol. Chem.* **270,** 22548–22555
27. Chen, I., Safe, S., and Bjeldanes, L. (1996) *Biochem. Pharmacol.* **51,** 1069–1076
28. Meng, Q., Yuan, F., Goldberg, I. D., Rosen, E. M., Auborn, K., and Fan, S. (2000) *J. Nutr.* **130,** 2927–2931
29. Hong, C., Firestone, G. L., and Bjeldanes, L. F. (2002) *Biochem. Pharmacol.* **63,** 1085–1097
30. Rahman, K. M., Aranha, O., Glazyrin, A., Chinni, S. R., and Sarkar, F. H. (2000) *Oncogene* **19,** 5764–5771
31. Sarkar, F. H., Rahman, K. M., and Li, Y. (2003) *J. Nutr.* **133,** 2434S-2439S
32. Rahman, K. M., Aranha, O., and Sarkar, F. H. (2003) *Nutr. Cancer* **45,** 101–112
33. Hudson, E. A., Howells, L. M., Gallacher-Horley, B., Fox, L. H., Gescher, A., and Manson, M. M. (2003) *BMC Cancer* **3,** 2
34. Sherr, C. J. (2000) *Harvey Lect.* **96,** 73–92
35. Sherr, C. J. (1996) *Science* **274,** 1672–1677
36. Hamel, P. A., and Hanley-Hyde, J. (1997) *Cancer Investig.* **15,** 143–152
37. Musgrove, E. A., Lee, C. S., Buckley, M. F., and Sutherland, R. L. (1994) *Proc. Natl. Acad. Sci. U. S. A.* **91,** 8022–8026
38. Sutherland, R. L., and Musgrove, E. A. (2002) *N. Engl. J. Med.* **347,** 1546–1547
39. Morgan, D. O. (1995) *Nature* **374,** 131–134
40. Geng, Y., Yu, Q., Sicinska, E., Das, M., Schneider, J. E., Bhattacharya, S., Rideout, W. M., Bronson, R. T., Gardner, H., and Sicinski, P. (2003) *Cell* **114,** 431–443
41. Su, T. T., and Stumpff, J. (2004) *Sci. STKE* **2004,** pe11
42. D'Hondt, L., Andre, M., and Canon, J. L. (2003) *N. Engl. J. Med.* **348,** 1063–1064
43. Akli, S., and Keyomarsi, K. (2003) *Cancer Biol. Ther.* **2,** S38–47
44. Kang, Y. (2003) *N. Engl. J. Med.* **348,** 1063–1064
45. Keyomarsi, K., Tucker, S. L., and Bedrosian, I. (2003) *Nat. Med.* **9,** 152
46. Keyomarsi, K., Tucker, S. L., Buchholz, T. A., Callister, M., Ding, Y., Hortobagyi, G. N., Bedrosian, I., Knickerbocker, C., Toyofuku, W., Lowe, M., Herliczek, T. W., and Bacus, S. S. (2002) *N. Engl. J. Med.* **347,** 1566–1575
47. Sebastian, B., Kakizuka, A., and Hunter, T. (1993) *Proc. Natl. Acad. Sci. U. S. A.* **90,** 3521–3524
48. Gu, Y., Rosenblatt, J., and Morgan, D. O. (1992) *EMBO J.* **11,** 3995–4005
49. Malumbres, M., and Carnero, A. (2003) *Prog. Cell Cycle Res.* **5,** 5–18
50. Keenan, S. M., Bellone, C., and Baldassare, J. J. (2001) *J. Biol. Chem.* **276,** 22404–22409
51. Brown, K. A., Roberts, R. L., Arteaga, C. L., and Law, B. K. (2004) *Breast Cancer Res.* **6,** R130–R139
52. Porter, D. C., Zhang, N., Danes, C., McGahren, M. J., Harwell, R. M., Faruki, S., and Keyomarsi, K. (2001) *Mol. Cell. Biol.* **21,** 6254–6269
53. Hong, C., Kim, H. A., Firestone, G. L., and Bjeldanes, L. F. (2002) *Carcinogenesis* **23,** 1297–1305
54. Staub, R. E., Feng, C., Onisko, B., Bailey, G. S., Firestone, G. L., and Bjeldanes, L. F. (2002) *Chem. Res. Toxicol.* **15,** 101–109
55. Lee, T. H., Chuang, L. Y., and Hung, W. C. (1999) *Oncogene* **18,** 4269–4274
56. Donovan, J. C., Milic, A., and Slingerland, J. M. (2001) *J. Biol. Chem.* **276,** 40888–40895
57. Pines, J. (1991) *Cell Growth Differ.* **2,** 305–310
58. Moore, J. D., Kornbluth, S., and Hunt, T. (2002) *Mol. Biol. Cell* **13,** 4388–4400
59. Moore, J. D., Yang, J., Truant, R., and Kornbluth, S. (1999) *J. Cell Biol.* **144,** 213–224
60. Kojima, T., Tanaka, T., and Mori, H. (1994) *Cancer Res.* **54,** 1446–1449
61. Yuan, F., Chen, D. Z., Liu, K., Sepkovic, D. W., Bradlow, H. L., and Auborn, K. (1999) *Anticancer Res.* **19,** 1673–1680
62. Jin, L., Qi, M., Chen, D. Z., Anderson, A., Yang, G. Y., Arbeit, J. M., and Auborn, K. J. (1999) *Cancer Res.* **59,** 3991–3997
63. Couillard, S., Gutman, M., Labrie, C., Belanger, A., Candas, B., and Labrie, F. (1998) *Cancer Res.* **58,** 60–64
64. Keyomarsi, K., O'Leary, N., Molnar, G., Lees, E., Fingert, H. J., and Pardee, A. B. (1994) *Cancer Res.* **54,** 380–385
65. Harwell, R. M., Porter, D. C., Danes, C., and Keyomarsi, K. (2000) *Cancer Res.* **60,** 481–489
66. Harwell, R. M., Mull, B. B., Porter, D. C., and Keyomarsi, K. (2004) *J. Biol. Chem.* **279,** 12695–12705
67. Jackman, M., Kubota, Y., den Elzen, N., Hagting, A., and Pines, J. (2002) *Mol. Biol. Cell* **13,** 1030–1045